Application of Strip Model to Edge Column-Slab Connections Loaded with Outward Eccentricity

Carrera, Bernardo; Lantsoght, Eva O.L.; Alexander, Scott D.B.

Publication date
2022

Document Version
Final published version

Published in
Design of Slabs for Serviceability and Punching Shear Strength

Citation (APA)
Carrera, B., Lantsoght, E. O. L., & Alexander, S. D. B. (2022). Application of Strip Model to Edge Column-Slab Connections Loaded with Outward Eccentricity. In M. Mahamid, & R. B. Gayed (Eds.), *Design of Slabs for Serviceability and Punching Shear Strength: Honoring Professor Amin Ghali 2020* (pp. 121-141). (American Concrete Institute, ACI Special Publication; Vol. SP-353). American Concrete Institute.

Application of Strip Model to Edge Column-Slab Connections Loaded with Outward Eccentricity

Bernardo Carrera, Eva O.L. Lantsoght and Scott D.B. Alexander

SYNOPSIS

The strip model describes a load path prior to failure that can be tailored to a wide range of slabs under concentrated loads, both concentric and eccentric. Eccentric punching shear can occur in concrete slab-column connections subjected to shear and unbalanced moment, such as edge and corner columns. This paper shows how the strip model is applied to experiments of edge column-slab connections tested with outward eccentricities, and compares this approach to the traditional and simplified ACI 318-19 approaches for dealing with eccentric punching shear. This work shows how a lower-bound plasticity-based model can be used for the practical case of the slab-column capacity for edge and corner columns, how it may explain the mechanics behind the ACI code provisions, and can help researchers identify adequate test setups for future experiments.

Keywords: arched strut, columns, eccentric punching shear, reinforced concrete, slabs, strip model

Bernardo Carrera is an undergraduate student in the Department of Civil Engineering at Universidad San Francisco de Quito, Quito, Ecuador. His research interests include cost-effective design of reinforced concrete structures under seismic activity, development of techniques regarding the evaluation and strengthening of existing structures as well as exploring the sustainability aspects related to concrete and construction.

ACI member **Eva O. L. Lantsoght** is a Full Professor at Universidad San Francisco de Quito, and an Assistant Professor at Delft University of Technology. She is the Vice Chair of ACI 445-0E Torsion, member of ACI 445-0D Shear Databases, ACI-ASCE 421, Design of Reinforced Concrete Slabs, ACI 342, Evaluation of Concrete Bridges and Bridge Elements, and ACI-ASCE 445, Shear and Torsion, and an associate member of ACI 437, Strength Evaluation of Existing Concrete Structures.

Scott D. B. Alexander, FACI, is a Professor of Practice in the Department of Civil and Environmental Engineering at the University of Alberta. He is an associate member of Joint ACI-ASCE Committees 421, Design of Reinforced Concrete Slabs, and ACI-ASCE Committee 445, Shear and Torsion, and its Subcommittee 445-C, Punching Shear. His research interests include structural applications of high-performance concrete, bridge rehabilitation, and punching shear.

INTRODUCTION

The strip model (Alexander, 2017) is a general design method for column-slab connections. It defines viable pathways for the transfer of load between slab and column. With suitable criteria to set the strength of these pathways, the result is a lower bound estimate of capacity (i.e. erring on the safe side). The key concept used in the strip model is an arched concrete compression strut. The arched strut models shear transfer in two-way slabs under a concentrated load. The strip model has been shown to give reliable predictions for the capacity of both interior and edge column-slab connections reported in the literature (Alexander, 2017).

In the case of edge column-slab connections, most experimental investigations of shear and moment transfer consider only moment about an axis parallel to the free edge of the slab. While the boundary conditions vary, every test set-up has a single axis of symmetry perpendicular to the free edge of the slab through the center of the column. Slab moments at the column support about axes perpendicular to the free edge are symmetric, hence termed “balanced,” and require no contribution from the column to satisfy equilibrium. Any slab moment at the column support about the axis parallel to the free edge must be equilibrated by bending in the column and is termed an “unbalanced” moment.

The ratio of the unbalanced moment to shear gives an eccentricity of loading. When the combination of shear and unbalanced moment results in negative or hogging moment in the slab (tension in the top slab reinforcement perpendicular to the free edge), the eccentricity is “inward” relative to the centroid of the column. When the combination of shear and unbalanced moment results in positive or sagging moment in the slab (tension in the bottom slab reinforcement perpendicular to the free edge), the eccentricity is “outward” relative to the centroid of the column. Testing at an outward eccentricity models a combination of gravity and lateral load where the lateral load is sufficient to reverse the sign of the moment transferred to the column.

Alexander (2017) demonstrates the application of the strip model to tests with inward eccentricity; however, that data set contains no results from specimens tested with an outward eccentricity. This paper presents results from applying the strip model to tests of thirteen edge connections reported by Albuquerque et al. (2016), ten of which featured specimens tested with outward eccentricity. The strip model is also compared to procedures for edge column-slab connections in ACI 318-19.

RESEARCH SIGNIFICANCE

The strip model describes viable load paths within the slab-column structural system. As a result, it provides more detailed insights into shear and moment transfer between a slab and column than can be obtained from conventional, code-based failure criteria. There are several benefits.

For experimenters:

- Load paths can be verified by detailed analysis and/or direct measurement (Alexander et al., 1995; Afhami et al., 1998).
- Design of laboratory tests can be more focused since there is a clearer picture of the active load paths.

For designers:

- The risk of an unsafe design is reduced in cases where the geometry and/or load combinations are outside the body of test results for which empirical code procedures have been tuned.
- There is guidance regarding the placement of flexural reinforcement and shear reinforcement.
- The analysis identifies locations where bond or anchorage are critical.

STRIP MODEL

The strip model describes the transfer of shear between a slab and column with a combination of arched concrete compression struts and one-way shear. Alexander (2017) presents a brief background of the development of the model and applies it to a number of tests of interior and edge column-slab connections reported in the literature. Alexander and Lantsoght (2018) show how the model easily adapts to the design of connections ranging from the conventional to the unusual.

ACI 318-19 recognizes strut and tie models as being appropriate for deep beams or disturbed regions at supports, sudden changes in geometry, or concentrated load points. The arched strut is a special case of the concrete compression strut that is possible only in regions with two-way bending behavior.

Commentary to Chapter 23 of ACI 318-19 describes D-regions and B-regions in one-way flexural elements such as beams or frames. In D-regions it is incorrect to assume a linear distribution of strain (plane sections) through the cross section. Shear transfer in a D-region is best described by strut and tie methods. B-regions are those where the assumption of a linear distribution of strain holds. In a B-region, shear strength is estimated using the one-way shear contribution of the concrete, which may be augmented by shear reinforcement.

The strip model applies the concepts of B- and D-regions to a two-way flexural system. An important difference between one- and two-way systems is that, in a two-way structure, there are mechanisms of shear transfer in two directions. A portion of slab may behave as a D-region in one direction and a B-region in the perpendicular direction.

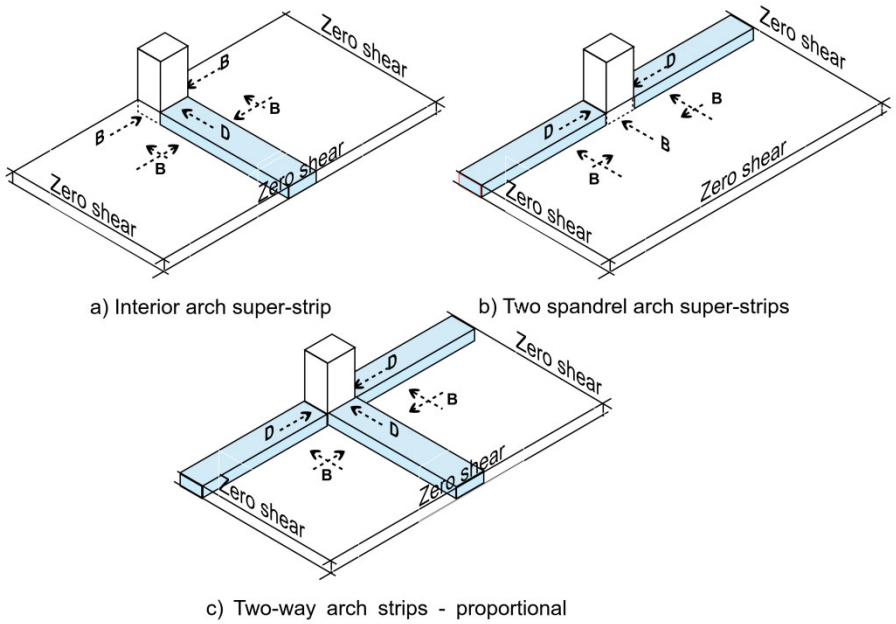

Figure 1: Typical layouts of arch strips at an edge column-slab connection

The slab is subdivided into the two-way equivalent of B-regions and D-regions, with the D-regions called arch strips. An arch strip is a strip of slab, parallel to the flexural reinforcement, supported at one end by a column (column end) and extending to the position of zero shear at midspan of the slab (remote end). The width of the arch strip is defined by the width of the column support. Within each arch strip, an arched strut carries vertical load from the slab to the column (i.e. acts as a D-region). Outside of the strip (including the direction perpendicular to the strip) shear transfer is by the two-way plate equivalent of beam action (i.e. acts as a B-region). For convenience, this will be referred to simply as beam action, with the fact that it is the two-way plate equivalent being understood.

Figure 1 shows three configurations of arch strips at an edge column-slab connection to transfer shear and moment about an axis parallel to the free edge. In Fig.1a, arching is in the direction perpendicular to the free edge. Shear transfer parallel to the free edge is by beam action. In Fig. 1b, arching is parallel to the free edge with shear transfer perpendicular to the free edge by beam action. The term "super-strip" is used for cases where arching is on one direction only, as in Fig. 1a and 1b. For arching in two directions, as illustrated in Fig.1c, the adjacent B-regions are transferring shears in two directions. Afhami et al. (1998) coined the term "proportional loading" to describe the particular case where arch strips in the orthogonal directions are loaded in proportion to their strength. The choice of configuration of arch strips depends on the loading eccentricity (or range of loading eccentricities) to be modelled.

Treatment of D-regions

Figure 2 shows the net loading on an arch strip, which defines the geometry of the arched strut acting within. At its column end, the arch strip delivers a shear, P_s and moment, $M_{s,col}$, to the column. At its remote end, the arch strip is loaded in moment only ($M_{s,rem}$). The side faces of the arch strip are loaded in beam action, limited by the one-way shear capacity of the slab, q_c. A factor χ accounts for cases where an arch strip is loaded more heavily on one side than the other. For an arch strip loaded equally on both sides, $\chi = 1$ (eg. Fig. 1a). For a strip loaded on one side only, as may be the case for a spandrel strip (eg. Fig. 1b) at an edge column slab connection, $\chi = 0$.

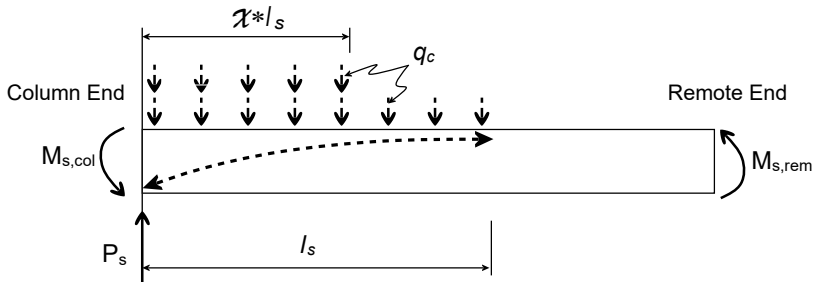

Figure 2: Arched compression strut within arch strip

The loaded length of the arched strut, l_s, is calculated from flexural equilibrium of the strip:

$$l_s = \sqrt{\frac{2M_s}{q_c(1+\chi^2)}} \tag{1}$$

where M_s is the sum of $M_{s,col}$ and $M_{s,rem}$ (Figure 2 shows positive orientation of $M_{s,col}$ and $M_{s,rem}$). It follows that the shear capacity of a single arch strip is given by:

$$P_s = q_c \times l_s(1+\chi) = \sqrt{\frac{2M_s q_c(1+\chi)^2}{1+\chi^2}} \tag{2}$$

Equation (2) requires values for two quantities: the loading term strength, q_c, and the flexural support of the arch strip, M_s. The loading term is estimated using the provisions for one-way shear in beams. The flexural support is based on conventional flexural mechanics.

The Loading Term, q_c

The ACI 318-19 expression for the concrete contribution to one-way shear includes factors for both size effect and reinforcement ratio.

$$V_c = 8\lambda_s\lambda\sqrt{f_c} \times \rho^{\frac{1}{3}} \times b_w d \qquad \text{(in-lb units)}$$

$$V_c = 0.67\lambda_s\lambda\sqrt{f_c} \times \rho^{\frac{1}{3}} \times b_w d \qquad \text{(SI units)}$$

where λ_s is a factor accounting for size, λ is a factor accounting for concrete density, and ρ is geometric mean of the reinforcement ratios in longitudinal and transverse directions.

Past work has shown (Alexander, 2017) that the contribution of flexural reinforcement is adequately accounted for in the formulations of the strip model. Including it in the one-way shear may be unnecessary. Alexander and Simmonds (1992) show that the factor of $\rho^{\frac{1}{3}}$ is not needed for lightly reinforced, concentrically loaded interior column-slab connections and leads to unconservative predictions for reinforcing ratios in excess of about 1.5%. It should be recognized that interior connections benefit from more confinement than do edge connections (or corner connections). As a result, it is prudent to reduce shear strength where reinforcement is light but potentially unsafe to count on any increase for values of ρ greater than about 1.5%. Hence, the value of $\rho^{1/3}$ is capped at 0.25, resulting in:

$$q_c = 8\lambda_s\lambda\sqrt{f_c}\times\rho^{\frac{1}{3}}\times d \quad \left(\leq 2\lambda_s\lambda\sqrt{f_c}\times d\right) \qquad \text{(in-lb units)} \qquad (3a)$$

$$q_c = 0.67\lambda_s\lambda\sqrt{f_c}\times\rho^{\frac{1}{3}}\times d \quad \left(\leq 0.17\lambda_s\lambda\sqrt{f_c}\times d\right) \text{ (SI units)} \qquad (3b)$$

The stepped nature of the loading diagram in Fig. 2 is a reasonable approximation of the combined effect of beam shear and torsion on the side faces of the strip after cracking and some localized yielding of flexural reinforcement (Afhami et al., 1998). It is also consistent with lower bound plasticity provided the mechanism generating the internal beam shear is sufficiently ductile. In the case of a two-way plate, it can be shown that load is brought to the side faces of the strip by beam-like slender shear but that shear is redistributed by torsional moment. This mechanism of redistribution does not exist in purely one-way systems. Maintaining the one-way concrete shear contribution throughout this redistribution is not different than the routine assumption in beam design that the concrete contribution to shear is additive with that of the shear reinforcement.

Flexural Support, M_s

The flexural support of an arch strip has two parts, $M_{s,col}$ and $M_{s,rem}$. The magnitude of $M_{s,rem}$ is given by the moment acting within the width of strip. In most cases of edge columns, the contribution of $M_{s,rem}$ is small and can be neglected with no great loss.

For a super-strip, as in Fig. 1a or 1b, the width of the strip matches the support but a wider band of reinforcement contributes to $M_{s,col}$, analogous to a T-beam in negative moment. Consistent with common design practice in North America, this wider band is taken to be the column dimension plus $1.5h$ on either side. This has been shown to give reasonable results (Alexander, 2017). For the case of proportional loading (Fig. 1c), the biaxial B- and D-regions constrain the band of reinforcement contributing to $M_{s,col}$ to the width of the column support.

While both $M_{s,col}$ and $M_{s,rem}$ are limited by the flexural reinforcement provided, it is possible that they may not reach this limit. The moment values for flexural support must be consistent with the loading. In design this is not a problem since the design moments come from the same load case that defines the design shear (Alexander and Lantsoght, 2018). In the analysis of test results, whether the moment values can reach full strength may need to be checked for consistency with the calculated shear capacity. It is possible that the slab has excess reinforcement that cannot be developed.

Figure 3 shows the assumed stress resultants acting at the interface between an edge column and the slab. A shear and moment of V_{tot} and M_{col} are transferred to the column. Under symmetric loading, the shears and moments on the spandrel faces (c_1 faces) are equal. Torsion is assumed to be zero on all faces unless there is some additional feature, such as closed hoops, that would develop torsion. For rotational equilibrium about an axis parallel to the free edge:

$$M_{col} = M_{face} + V_2 \times \frac{c_1}{2} \qquad (4)$$

Figure 4 shows the typical shape of a capacity envelope for an edge column-slab connection using the three arch strip configurations shown in Fig. 1 and ignoring the contribution of $M_{s,rem}$. Figure 1a describes the arch strip configuration that generates segment A to A' of the capacity envelope. Figure 1b illustrates the arch strip configuration responsible for D to B to B' of the capacity envelope. Figure 1c describes the arch strip configuration for A to C to D.

It is convenient to distinguish the transverse direction of shears and arched struts. A gravity-oriented shear or arch strip is one that transfers to the column a vertical load that is consistent with gravity. An uplift-oriented shear or arch strip delivers a load in the opposite direction. For convenience, the word "oriented" is taken as understood.

At point A, a fully-developed interior super-strip combines with gravity shear on the spandrel (c_1) faces of the column. At point C, fully-developed spandrel super-strips are combined with maximum one-way gravity shear and positive moment acting on the interior (c_2) column face. Point C gives the shear and moment resulting from

proportional loading, where arching equally developed in both directions and the flexural reinforcement supporting those arches is limited to that passing through the column.

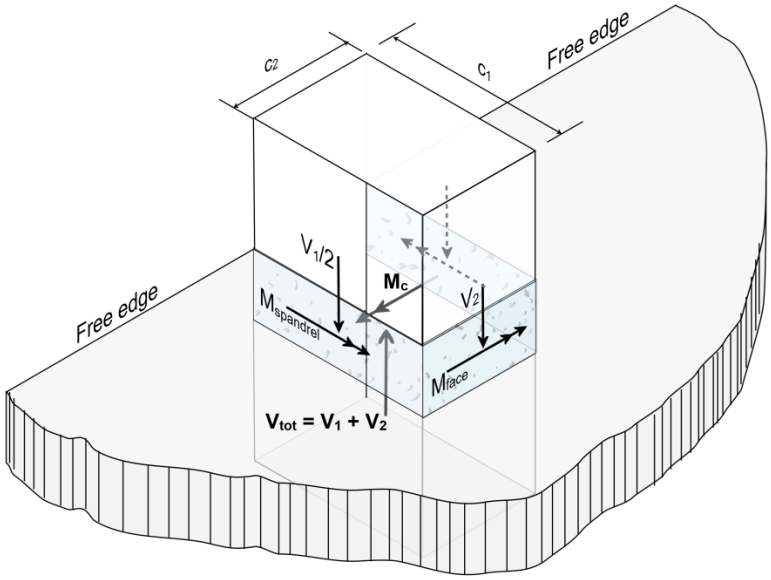

Figure 3: Shears and moments at an edge column-slab connection

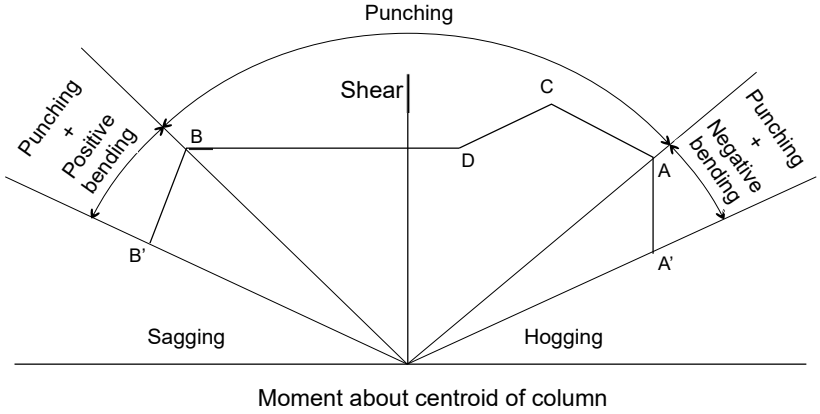

Figure 4: Capacity envelope at edge column -moment about axis parallel to free edge

The shear plateau between point B and point D is defined by varying the flexural moment acting on the interior face, M_{face} (see Fig. 3), from its maximum positive value to a transition value marking the change from one-way shear to arching on the inside face.

The secondary points, A' and B', result from shear reversal for the column faces loaded in one-way shear. Point A' combines a gravity arch super-strip on the inside face with uplifting one-way shear on the spandrel faces. Point B' is the combination of gravity arch super-strips on the spandrel faces combined with uplifting one-way shear and maximum positive moment on the inside face.

Connections failing at shear-moment combinations falling between A and B are reaching a shear limit of some kind. From A to A' the connection is governed primarily by negative bending. From B to B' the connection has reached a limit on positive moment.

It is convenient to introduce some notation.

P_s, l_s, M_s : Strip model quantities of load, loaded length, and moment capacity associated with a proportionally loaded arch strip. Band of reinforcement providing flexural support is limited to width of column support.

P_{ss}, l_{ss}, M_{ss} : Strip model quantities of load, loaded length, and moment capacity associated with a super-strip. Band of reinforcement providing flexural support is the width of column support plus 1.5h on either side.

Additional subscripts of 1 or 2 will indicate quantities associated with the spandrel or interior faces, respectively.

ANCHORAGE OF REINFORCEMENT

Anchorage of reinforcement may limit the flexural capacity of a strip perpendicular to the free edge. Top reinforcement passing through the column typically has adequate anchorage. These bars are usually hooked and are well confined (even clamped) by the column. Bars passing through the column might still be critical in anchorage if there is little confinement, as is the case for a roof slab, or if the column dimension perpendicular to the free edge is small compared to the development length, hooked or straight, of the bars in tension.

Figure 5 illustrates an approach for estimating the effectiveness (anchorage) of bars outside the column. This method has been shown to be in reasonable agreement with tests (Alexander, 2017). A sloping line on either side of the column defines the region within which a reinforcing bar is considered at least partially effective. Bars A and B are within this region and would contribute to the moment capacity of a super-strip perpendicular to the free edge of the slab. Since Bar C is outside this region, it would be ineffective as reinforcement for a super-strip.

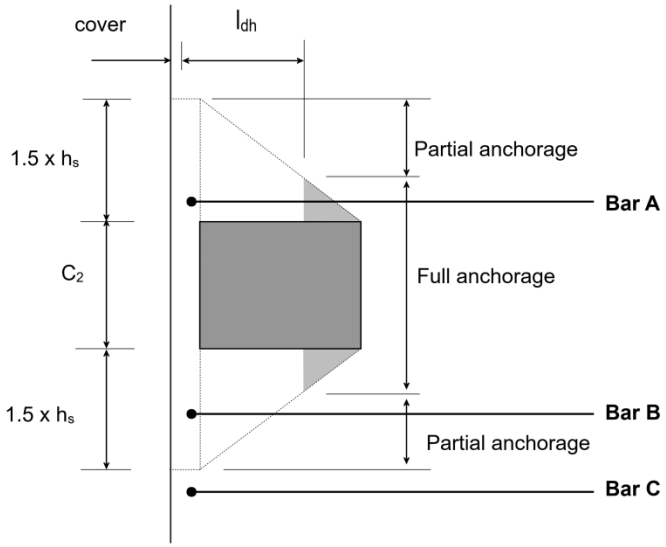

Figure 5: Anchorage of reinforcement perpendicular to a free edge

Bars A and B both contribute to $M_{s,col}$, but they are not equally effective. The embedment of Bar A beyond the sloping line exceeds the hook development length, l_{dh}; hence, it is fully anchored. Bar B does not have sufficient embedment for full anchorage. The force associated with Bar B must be reduced to account for this.

For steel reinforcement with bar sizes, cover, and spacing that are typical in slabs, the hook development length is about one-half of the straight bar development length. This implies that the hook provides mechanical anchorage for about one-half of the yield bar force. It follows that the available tensile force for hooked bars within the region of partial anchorage varies linearly from full to half yield. Of course, if the bars perpendicular to the free edge are not hooked, their effectiveness will be reduced substantially.

APPLICATION OF STRIP MODEL TO TESTS WITH OUTWARD ECCENTRICITY

Outline of tests by Albuquerque et al.

Albuquerque et al. (2016) report results from thirteen edge column-slab specimens tested at different eccentricities (ratio of moment to shear). Figure 6 shows the typical test specimen. The slabs measured 2350 mm × 1700 mm × 180 mm (92.5 in × 66.9 in × 7.1 in) with a 300 mm (11.8 in) square edge column stub at one end. For each test, the position of the point support was fixed relative to the centroid of the column, thereby controlling the eccentricity of that test (positive eccentricity shown in Fig. 6). A boot on the column stub allowed the point support to be positioned outside the column cross section. With the point support under the edge column stub and the line support

at the opposite end, each test was simply supported with a span length of 2000 mm (6.56 ft) plus the value of eccentricity for that test. Equal point loads were applied at four locations.

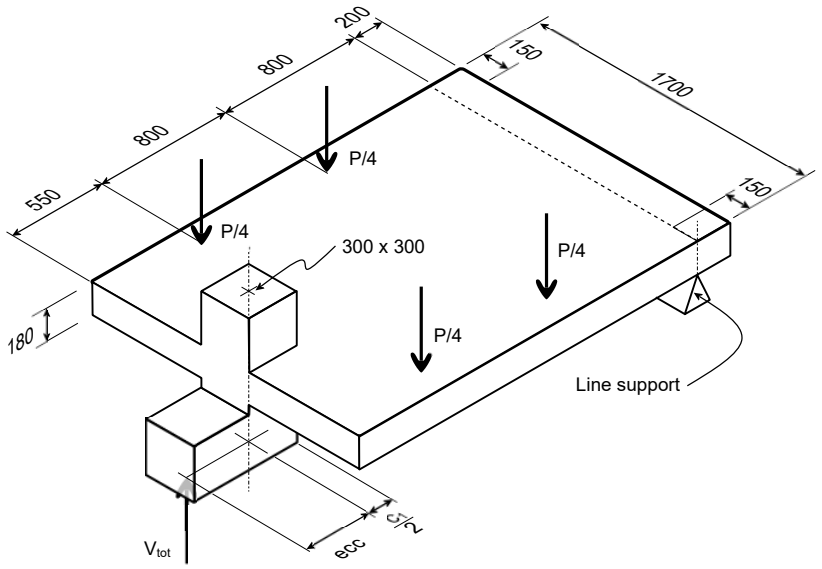

Figure 6. Slab specimens tested by Albuquerque et al. (2016). Units: mm. Conversion: 1 mm = 0.04 in.

The main variables in these experiments are the support eccentricity and the bottom flexural reinforcement perpendicular to the free edge (Standard or Enhanced). The standard reinforcement layout is designed to study a punching failure close to the flexural capacity and the enhanced reinforcement layout contains more bottom flexural reinforcement. Two specimens include studs as shear reinforcement and two specimens have closed hoops to provide torsional reinforcement for the spandrel strips.

Appendix A gives an overview of the main properties of the tested slabs, as well as the most important results of these experiments.

Strip model analysis

To generate a capacity envelope, shear and moment capacities required in Equation (2) are needed. Table 1 presents the results of these calculations for all of the tests reported by Albuquerque et al. (2016). These are grouped according to the reinforcing configuration of the specimens. Reported averages for both "Standard" and "Enhanced" reinforcement are calculated using the average reported concrete strength for that group. For the six specimens with Standard reinforcement, that average is 47.7 MPa (6,918 psi) while the average strength of the three specimens with Enhanced reinforcement is 46.2 MPa (6,701 psi).

Table 1: Calculated quantities for strip model. Conversion: 1 kN·m = 0.74 kip·ft; 1 kN/m = 0.07 kip/ft.

		Interior Strip (top steel)		Interior Strip (bottom steel)		Spandrel Strip (top steel)		
Test	**Reinf. Config.**	M_{s2} (kN·m)	M_{ss2} (kN·m)	M_{s2} (kN·m)	M_{ss2} (kN·m)	M_{s1} (kN·m)	M_{ss1} (kN·m)	q_c (kN/m)
Average	**Std.**	**26.9**	**54.5**	**44.5**	**84.8**	**44.5**	**69.0**	**155**
Average	**Enh.**	**26.9**	**54.3**	**57.0**	**105.2**	**44.3**	**68.6**	**162**
L9	**Std. + Studs**	**27.2**	**56.2**	**45.3**	**89.1**	**45.3**	**71.2**	**170**
L10	**Enh. + Studs**	**27.2**	**56.4**	**58.9**	**116.4**	**45.4**	**71.5**	**184**
L8	**Enh. + Hoops***	**27.0**	**55.1**	**57.7**	**95.7**	**44.7**	**69.7**	**170**
L13	**Enh. + Hoops***	**26.8**	**53.8**	**56.6**	**102.9**	**44.1**	**67.9**	**158**

*Moment capacities do not include contribution of torsion reinforcement

An important detail for these tests is that both top and bottom reinforcement perpendicular to the free edge of the slab had 180-degree hooks. As a result, anchorage of both top and bottom reinforcement contributing to different values of M_{s2} was excellent.

Specimens L9, L10, L8, and L13, have additional reinforcing features that require special attention. Specimens L8 and L13 contain torsion reinforcement while specimens L9 and L10 contain stud shear reinforcement. The contributions from this reinforcement will be treated separately.

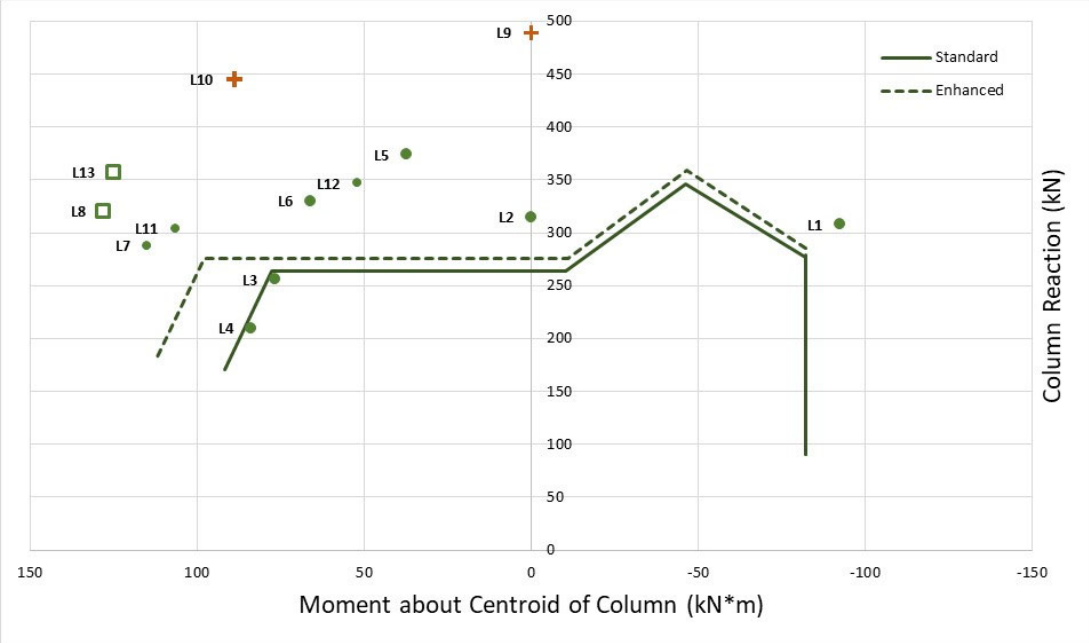

Figure 7. Shear-moment capacity diagrams with experimental results by Albuquerque et al. (2016). Conversion: 1 kN = 0.225 kip; 1 kN·m = 0.74 kip·ft

Figure 7 shows load and moment test results for all specimens reported by Albuquerque et al. (2016) as well as capacity envelopes according to the strip model for both "Standard" and "Enhanced" reinforcement (no transverse reinforcement), calculated using the corresponding average values in Table 1. Appendix A provides detailed calculations for the capacity envelope for the "Standard" reinforcement case.

The capacity diagrams shown in Fig. 7 follow the form of the conceptual diagram shown in Fig. 4. The load transfer mechanisms described for points A, A', B, B' and C in Fig. 4 can be applied to the tests. To do this, consider where a line from the origin to a data point crosses the capacity diagram. For reference, in Fig. 7 lines are drawn from the origin to point A on the Standard capacity diagram and point B on the Enhanced capacity diagram.

The test result for L1 is on the boundary between being critical in punching and critical in negative bending (as defined in Fig. 4). This combination of shear and moment is typical at an edge connection under maximum gravity load. An interior super-strip carries maximum shear and negative moment to the edge column. It is worth noting that, for this test program, this and L2 are the only specimens for which the strip model capacity would be affected by including the flexural support at the remote end of the arch strip.

Specimens L2, L5, L6, and L12 are all governed by the shear capacity of spandrel super strips plus one-way shear on the c_2 face of the column. The flexural moment to be transferred to the column is as required by equilibrium but within the limits of capacity dictated by reinforcement perpendicular to the free edge. In all cases, Equation 1 gives a value of l_s that is too long to fit within the specimen. As a result, the capacity is controlled by the one-way shear limit across the full width of the test specimen.

Specimens L3 and L11 lie almost exactly on the expected boundary between shear failure and bending failure defined in Fig. 4. L3 is reported to have a flexural failure; L11 failed prematurely at a loading point. Specimens L4 and L7 are controlled by the maximum positive moment that can be anchored to the column. Both are reported to have flexural failures.

These nine specimens with no shear reinforcement have values of average ratio of test load to expected capacity ranging from 1.00 to 1.37. This is well within the range of results reported previously (Alexander, 2017) for

the strip model. More importantly, the strip model gives insight into what drives the different observed failure modes in the experiments.

Contribution of stud reinforcement (L9 and L10)

Specimens L9 and L10 have the radial layout of stud reinforcement shown in Fig. 8. Specimen L9 has a "Standard" layout of flexural reinforcement while L10 has an "Enhanced' layout. The studs have a diameter of 8 mm (0.32 in) and a yield strength of 587 MPa (85,140 psi). The dimensions are based on the following:

- All studs are on lines that are centered on the column
- The angle between adjacent stud lines is 30 degrees
- The first stud in each line is 70 mm (2.8 in) from the column face
- Each line of studs is 300 mm (11.8 in) long

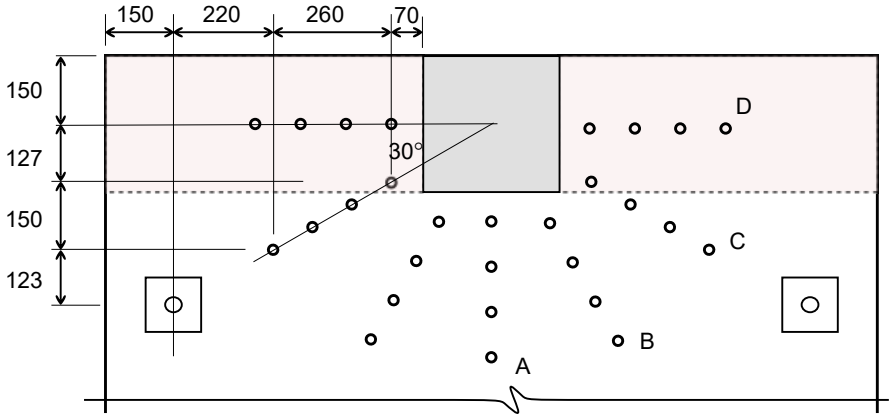

Figure 8. Layout of stud reinforcement (Albuquerque et al. 2016). Units: mm. Conversion: 1 mm = 0.04 in.

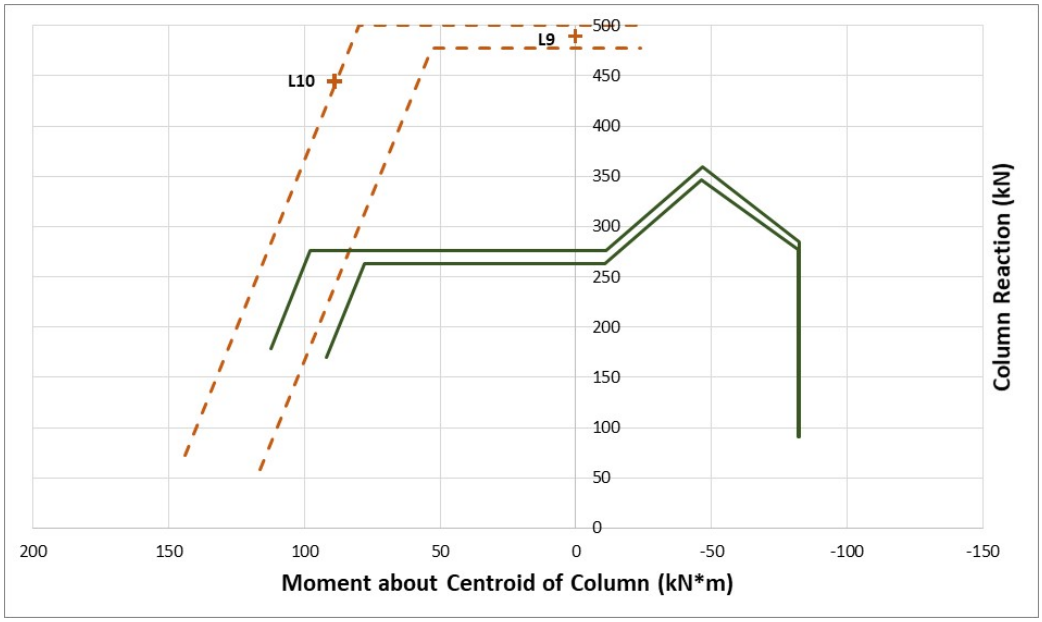

Figure 9. Shear-moment capacity diagrams with specimens with stud reinforcement. Conversion: 1 kN = 0.225 kip; 1 kN·m = 0.74 kip·ft

Using ACI 318-19, the contribution of shear reinforcement in a B-region is given as:

$$V_s = \frac{A_v f_{yt} d}{s} \quad (5)$$

where A_v, f_{yt}, and s are the area, yield strength and spacing of the shear reinforcement and d is the flexural depth of the member. Equation (5), developed for shear capacity of transverse reinforcement in the B-region of a beam, is

easily adapted to a line of stud reinforcement but it is appropriate only if those studs lie within B-regions. For these tests, the potential contribution for any line of studs is 43.1 kN (9.7 kip).

The active D-region for both L9 and L10 is shown as shaded in Fig. 8 while the B-region is unshaded. Stud lines A and B are fully effective since they are wholly within the two-way B-region, with each contributing additional capacity of 43.1 kN (9.7 kip). Stud line D, entirely within the spandrel D-region, makes not contribution to shear capacity at these loading eccentricities.

The positioning of stud line C makes its behavior ill-defined. It straddles the boundary between B- and D-region and is more closely aligned with the spandrel super-strip. Here it will be assumed that the stud line is indirectly supported by the spandrel arch, with the stud closest to the column acting as a hanger. This limits the capacity of stud line C to 29.5 kN, the yield strength of the hanger.

Fig. 9 shows test values and partial capacity envelopes for specimens L9 and L10 as well as the base envelopes for Standard and Enhanced reinforcement from Fig. 7. Both are reported to have shear failures in the loading apparatus rather than failures of the connection. The predicted connection capacities are on the safe side.

Contribution of torsional reinforcement (L8 and L13)

To add torsional resistance, the spandrels or specimens L8 and L13 were furnished with closed ties having outside dimensions of 250 mm by 140 mm (9.8 in × 5.5 in) and spaced at 60 mm (2.5 in) on center on the spandrels. For L8, the ties had a diameter or 8 mm (0.32 in) and yield strength of 587 MPa (85,140 psi). For L13, the tie diameter was reduced to 6.3 mm (0.25 in) with a reported yield strength of 580 MPa (84,120 psi).

The method to estimate torsion capacity outlined in Chapter 22 of ACI 318-19 is based on a space truss analogy that requires a design angle of compression field of between 30° and 60°. The larger of these angles is assumed here as it produces a smaller torque and produces the least demand for axial force; hence, the unfactored torsional capacities for the 6.3 mm (0.25 mm) and 8 mm (0.32 in) ties are 11.0 kN·m (8.1 kip·ft) and 17.4 kN·m (12.8 kip·ft), respectively.

An additional complication is that the layouts of bottom reinforcement perpendicular to the free edge for specimens L8 and L13 are not the same. The reinforcement for L13 exactly matches that of the specimens with "Enhanced" reinforcement (L7, L11, L12). Specimen L8 has a modified layout of reinforcement, reducing the magnitude of M_{ss2} relative compared to that of specimen L13 (see Table 1).

Figure 10 shows the reported test loads and corresponding partial capacity diagrams incorporating the additional torsional strength provided by closed ties in the spandrels. For reference, the capacity diagram for Enhanced reinforcement from Fig. 7 is shown. As was the case for specimens with stud reinforcement, the strip model provides conservative estimates of capacity.

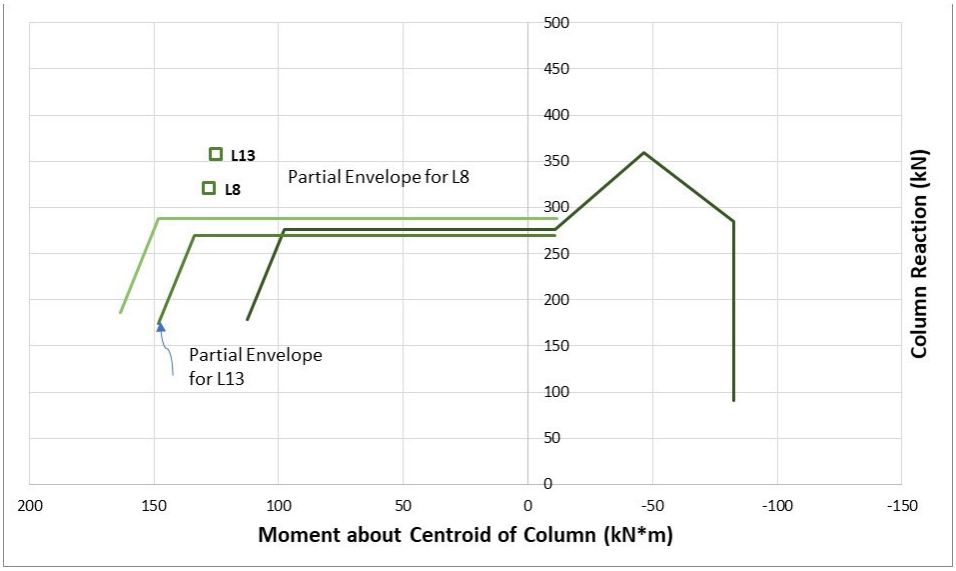

Figure 10. Shear-moment capacity diagrams with specimens with hoops. Conversion: 1 kN = 0.225 kip; 1 kN·m = 0.74 kip·ft

The shear capacities of the plateaus for the partial diagrams vary slightly from that of the full capacity diagram owing to differences in concrete strength. The main effect of additional torsional strength is to extend the plateau to the left. For specimen L8, the net effect from the addition of closed ties and the change in reinforcing layout is an increase in positive moment capacity of approximately 25 kN·m (18.4 kip·ft) relative to the "Enhanced" reinforcement capacity diagram. In the case of specimen L13, the closed ties provide an additional capacity of approximately 22 kN·m (16.2 kip·ft).

Effect of bottom reinforcement (continuity)

Figure 11 shows the effect of accounting for positive moments in the slab. Up till now, the capacity interactions have been based on flexural support to arch strips provided at the column end. For any load distributions involving an interior arch strip (as in Fig. 1a or 1c), the positive moment at midspan contributes to the flexural support of the arch strip. Because these test specimens are statically determinate, this positive moment contribution can be calculated for any given load and testing eccentricity. The shear and moment combinations for points A, C, and D of the capacity interaction are calculated using an iterative procedure. As can be seen in Figure 11, adding the effect of the bottom reinforcement increases the predicted shear capacity using the strip model and provides a closer estimate for experiments L2 and L1, but the approach becomes computationally more cumbersome.

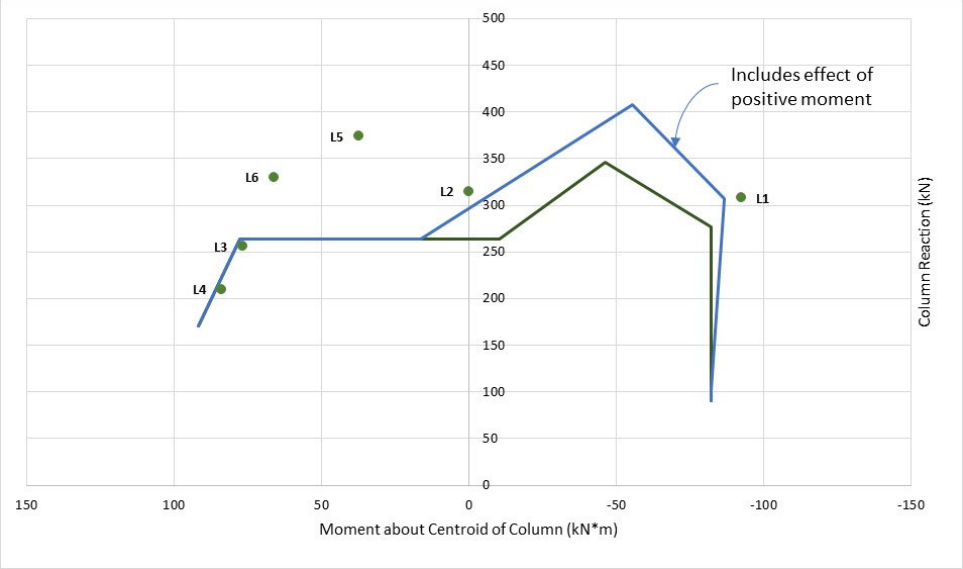

Figure 11. Effect of including flexural support at remote end of strip. Conversion: 1 kN = 0.225 kip; 1 kN·m = 0.74 kip·ft

COMPARISON OF STRIP MODEL AND ACI CODE

Code Provisions for Eccentric Punching Shear

Historically, the ACI Code has considered an interaction equation that results from limiting a calculated shear stress on an assumed critical section. Moment transfer between slab and column is presumed to generate a non-uniform distribution of shear stresses that adds to a uniform distribution associated with vertical load. A maximum shear stress is calculated for any combination of net shear and net moment transferred to the column, and this calculated shear stress is compared to a limiting value. The resulting interaction equation is:

$$v_u = \frac{V_u}{b_o d} \pm \frac{\gamma_v M_{cs} c}{J_c} \quad (6)$$

where V_u is the factored shear acting on the centroid of the critical section; b_0 is the total perimeter of the critical section; c is the distance from the centroid of the critical section to the point where the shear stress is calculated; J_c is a section property of the critical section, analogous to a polar moment of inertia, and; $\gamma_v M_{cs}$ is the fraction of factored moment, taken about the centroid of the critical section, transferred by shear stresses acting on the critical section.

The full definitions of the terms in Equation 6 are provided in ACI 318-19 and will not be repeated here. However, it is important to note that the term γ_v is defined indirectly as $1-\gamma_f$ where $\gamma_f M_{cs}$ is the fraction of moment about the centroid of the critical section to be carried by flexure.

Figure 12 is a schematic representation of the complete interaction for shear and moment that results from applying Equation 6 at an edge column-slab connection. The moment is about an axis parallel to the free edge of the slab. Each corner of the four-sided interaction is defined by a critical stress state being reached simultaneously at both the inside face of the critical section and the free edge.

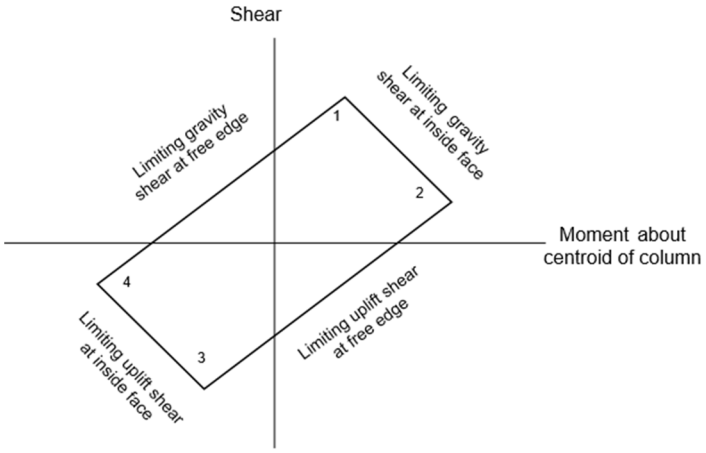

Figure 12: ACI 318 shear-moment interaction equation at edge-column slab connection

ACI 318-95 introduced a more flexible design approach under which the designer is permitted to assign a higher fraction of moment transfer to direct flexure with a corresponding smaller fraction to eccentric shear stresses and reduce the calculated shear stresses resulting from unbalanced moment so long as the vertical shear to be transferred met certain limits. ACI 318-19 permits $\gamma_f = 1$ (and hence, $\gamma_v = 0$) provided the average shear on the critical section is less than 75% of the maximum permissible.

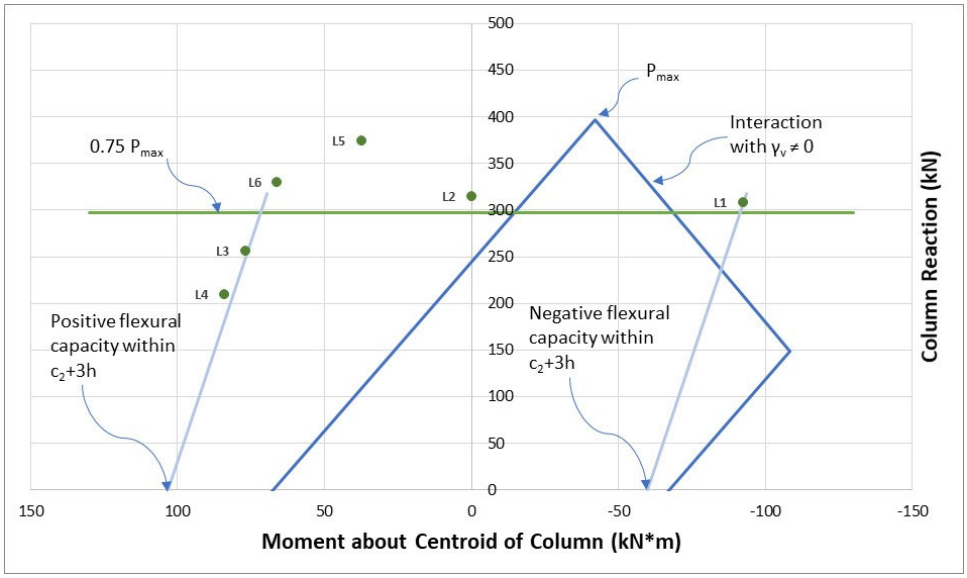

Figure 13: Combined design envelope using ACI 318-19 for standard reinforcement of Albuquerque tests. Conversion: 1 kN = 0.225 kip; 1 kN·m = 0.74 kip·ft

It is possible to combine the traditional interaction equation (Fig. 12) that uses fixed values of γ_f and γ_v with the more flexible design approach permitted under ACI 318-19. The result of applying this composite interaction to the average test specimen with Standard reinforcement is shown in Fig. 13.

A horizontal line at 75% of the peak value, P_{max}, of the traditional interaction is combined with flexural limits that are defined by reinforcement perpendicular to the free edge within a band of width c_2+3h. The lines defining the flexural limits are not vertical because the axial load is assumed to act at the centroid of the critical section. The slope of the flexural limit lines is 1/(distance between centroids of column and critical section). Using the envelope of the traditional interaction equation and the design approach with γ_F = 1 results in a composite interaction diagram that combines the limits for the positive flexural capacity, 0.75P_{max}, the traditional P_{max} line, the negative flexural capacity limit, and the negative flexural capacity limit from the traditional interaction diagram.

Comparison between ACI interaction envelope and strip model

Figure 14 compares the composite envelope of limiting shear and moment combinations defined by ACI 318-19 with the capacity envelope developed using the strip model for the standard reinforcement case of the Albuquerque experiments. The parallels between these two envelopes are remarkable.

Where the ACI 318-19 envelope has been able to stand the test of time, the strip model provides an understanding of the mechanics that govern the shear-moment interaction in slab-column connections. Both approaches show the limits related to the flexural capacity bounds; however, the strip model is not extended to the point of zero column reaction because the load cases that would produce such combinations of shear and moment are not clearly defined. Both approaches show a plateau in the negative moment region, which has been explained by the strip model as the influence of the varying flexural moment acting on the interior face of the column. Both approaches show a peak in shear capacity for the positive moment region, which is explained by proportional loading and the activation of three arched struts in the strip model.

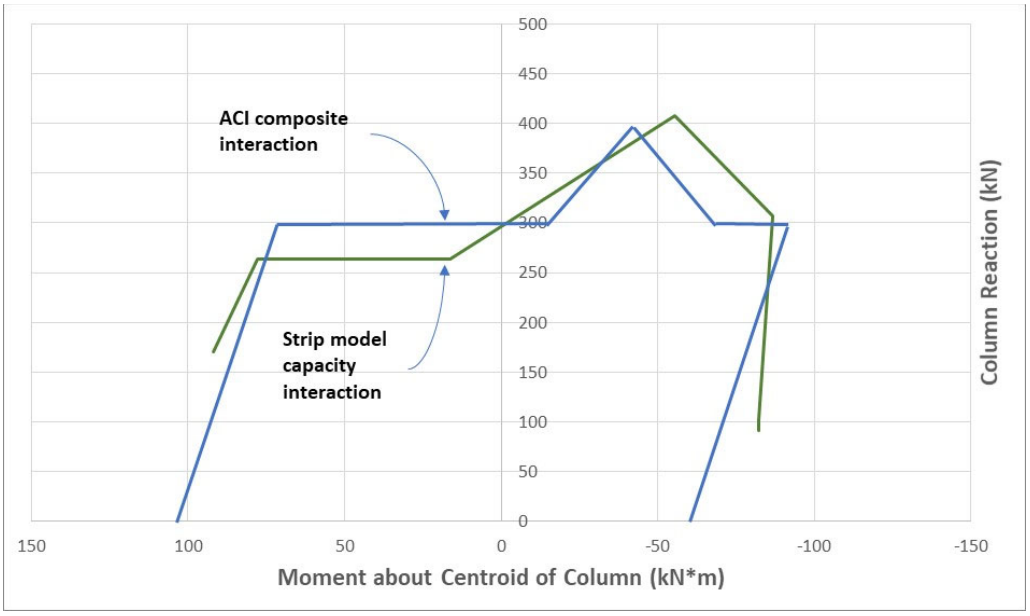

Figure 14: Comparison between ACI composite interaction diagram and strip model. Conversion: 1 kN = 0.225 kip; 1 kN·m = 0.74 kip·ft

DISCUSSION

As is now routinely done for one-way frame elements, the strip model subdivides a slender, two-way flexural element into B- and D-regions. What is different is that the definition of B- and D-regions in a two-way system must consider two directions. Each D-region has a geometry that is defined by its interaction with adjacent B-regions. The arched strut, a new device in the strut and tie tool kit, is the consequence of this interaction.

The analysis and limiting capacities used in the strip model are analogous to those that are used in the design of any one-way frame element. The analysis is simply to satisfy static equilibrium. Arched struts carry shear within D-regions. These struts are tied with flexural reinforcement, but for convenience this is expressed as flexural

support for the arch strip rather than tie forces. The limiting shear capacity in a B-region is given by the one-way shear strength, which may be augmented through the use of transverse shear reinforcement.

The magnitudes of bending moments are capped on the basis of available reinforcement but, as is always the case with strut and tie modelling, they must also be statically consistent with the shear. There is an important subtlety here that is especially important for design. The addition of flexural reinforcement will not necessarily increase shear strength. A better approach is to consider that the strip model provides guidance for the lateral distribution of a given flexural design moment that is consistent with a given design shear rather than a call for additional reinforcement.

Note that the one-way strength, a fundamental limit for shear transfer in one-way B-regions, is used without modification for two-way. The beam shear capacity used here is as defined in ACI 318-19, but with a limit to the longitudinal reinforcement term. No special two-way shear strength is needed. Slender reinforced concrete elements have a slender shear strength that is the same whether the system is one or two-way.

As is the case with results reported in previous studies, the strip model provides reliable estimates of the capacity of edge column-slab connections with no shear reinforcement. Here the specimens are tested with outward eccentricities. The contribution of flexural continuity is evident. While continuity can introduce complication in the analysis of test results, it poses no such problem in design since the designer will have, for every load case, a complete set of design shears and moments that are statically consistent.

The application of the strip model to specimens with shear reinforcement is straightforward because the model derives from a subdivision of B- and D-regions that follows from observed behavior. In a B-region, shear reinforcement will add shear capacity, but in a D-region it will not. For most load cases, it is a matter of first identifying which shear reinforcing elements are effective and then determining a full load path that is consistent with the already defined B- and D-regions.

The composite ACI interaction presented here agrees very well with these test results. The traditional ACI code approach, with a fixed value of $\gamma_V \neq 0$, is overly conservative for cases with outward eccentricity. The composite ACI interaction, at least for this series of tests, results in estimates of capacity that are much closer to the experimental results.

The comparison between the strip model and the composite ACI design interaction is striking. Both agree closely with test results; however, the strip model is based on an analysis of the load paths at the slab-column connection, and provides a mechanical understanding of how load is carried for different combinations of bending moment and shear. The composite envelope of the two ACI code approaches is based on no consistent model of behavior.

Because the strip model is an integration of consistent and verifiable load paths, it can be extrapolated with some confidence to more unusual problems. With respect to edge column slab connections, the literature is dominated by tests with unbalanced moments about the axis parallel to the free edge of the slab. The connections themselves usually have an axis of symmetry perpendicular to the free edge. This body of test results is the basis for which empirical code provisions have been developed; however, in practice the designer is likely to face cases where the geometry and/or load combinations are well outside this body of data.

Finally, the strip model gives insights that can guide experimental design. For example, the basic arched strut load path has been verified by detailed analysis and direct measurement (Alexander et al., 1995; Afhami et al., 1998). The understanding of internal load paths can help in developing more focused questions to be answered by experiments. One such question is the relative merits of distributed, radial and cruciform shear reinforcement. Another might be the limits, if any, on lateral distribution of design moment to influence shear strength.

SUMMARY AND CONCLUSIONS

The strip model provides the designer with a clear picture of how load is carried within a column-slab connection. It is an extension of strut and tie modelling for application to two-way flexural elements. It makes use of basic design concepts already recognized in the ACI code, adding only one, the arched strut. The arched strut is a special type of concrete compression strut that is unique to slender, two-way flexural systems. As is the case for any strut and tie model, satisfying equilibrium is fundamental.

With the exception of the arched strut, this picture is comprised of design elements and concepts already firmly established in the ACI code. Each part of the interaction diagram is derived from a unique set of load transfer mechanisms, so that the designer can also see in detail how the capacity of the connection is affected by changes in reinforcement or geometry. The model also gives meaningful guidance to the placement of enhancements such as shear reinforcement.

The strip model describes column-slab connection behavior with a combination of a one-way shear limit and localized arching behavior. In this work, we apply the Strip Model to eccentric punching shear experiments

carried out by Albuquerque and compare the resulting moment-shear capacity diagram to the ACI 318-19 interaction diagram. The strip model can also be used to include the effect of shear reinforcement as present in two experiments, as well as the effect of torsional hoop reinforcement, as present in two experiments.

For the ACI 318-19 code predictions, we observed that the traditional interaction diagram leads to a conservative prediction of the Albuquerque experiments, and that in particular the experiments with outward eccentricity are greatly underestimated. Combining the traditional approach with more recently added provisions, also in ACI 319-19, for using γ_F = 1, results in a moment-shear envelope in excellent agreement with the experimental observations. Remarkably, the composite ACI interaction diagram matches the capacity interaction developed for these specimens using the strip model. Further research is needed to explore the general validity of this correspondence between both approaches.

This research shows again the versatility of the strip model in dealing with a complex loading situation, in addition to cases that were studied in the past with the strip model (concentric and eccentric punching shear, approach slabs, slab bridges etc.). As such, the strip model can be a powerful tool for both designers and researchers: understanding the load paths that occur in slabs can aid designers in selecting the optimal reinforcement layout as well as analyzing design situations that are complex in geometry and loading, and this understanding can be valuable for researchers in the design of valuable experiments, as well as in identifying relevant positions for instrumentation during an experiment.

REFERENCES

ACI Committee 318, 1995, "Building code requirements for structural concrete (ACI 318-95) and commentary," American Concrete Institute; Farmington Hills, MI.

ACI Committee 318, 2019, "Building code requirements for structural concrete (ACI 318-19) and commentary," American Concrete Institute; Farmington Hills, MI, 503 pp.

Afhami, S., Alexander, S. D. B. and Simmonds, S. H., 1998, "Strip model for capacity of slab-column connections," Dept. of Civil Engineering, University of Alberta; Edmonton, xxi, 231 p. pp.

Albuquerque, N. G. B., Melo, G. S. and Robert, L. V., 2016, "Punching Shear Strength of Flat Slab-Edge Column Connections with Outward Eccentricity of Loading," *ACI Structural Journal*, V. 113, No. 05, 9/1/2016.

Alexander, S.D.B., 2017. "Shear and Moment Transfer at Column-Slab Connections," *ACI SP-315: ACI-fib International Symposium - Punching Shear of Structural Concrete Slabs*. pp. 1-22.

Alexander, S.D.B., Xilin Lu, and Simmonds, S.H. 1995. "Mechanism of Shear Transfer in a Column-Slab Connection," *1995 Annual Conference of the Canadian Society for Civil Engineering, Proceedings*, Ottawa, Ontario, Vol. II, pp. 207-216.

Alexander, S. D. B. and Simmonds, S. H., 1992, "Bond Model for Concentric Punching Shear," *ACI Structural Journal*, V. 89, No. 3, pp. 325-334.

Alexander, S. D. B. and Lantsoght, E. O. L., 2018, "The Arched Strut - a Tool for Modelling Column-Slab Connections," *IABSE 2018*, Nantes, France.

APPENDIX A

Reported test results (Albuquerque et al., 2016)

This provides a brief summary of specimen details for the tests reported in Albuquerque et al. (2016). The flexural reinforcement consists of diameters 12.5 mm (≈ #4 bar) and 16 mm (≈ # 5 bar) with yield strength measured as 530 MPa (76.9 ksi) and 558 MPa (80.9 ksi), respectively.

Table A1 provides a summary of reported observations, measurements, and test results. Some of the reported failure modes require further explanation. The "shear" mode reported for specimens L9 and L10 refers to a failure of the loading apparatus near the roller support under the column. The "local" failure mode refers to a failure at one of the loading points. Neither of these constitutes a failure of the column-slab connection. It is not known how much more load the connections might have carried were it not for these premature failures.

Table A1. Overview of test observations. Conversion: 1 mm = 0.04 in, 1 MPa = 145 psi, 1 kN = 0.225 kip.

Test	d (mm)	ρ (%)	$f_{c,avg}$ (MPa)	ecc (mm)	Mode Reported	P_{exp} (kN)	V_{exp} (kN)
L1	147	0.96	46.8	-300	punch	437	308
L2	146	1.24	44.7	0	punch	525	315
L3	146	1.24	45.1	300	flex	490	256
L4	146	1.24	46.0	400	flex	420	210
L5	146	1.24	51.4	100	punch	654	374
L6	146	1.24	52.1	200	punch	605	330
L7	146	1.49	50.0	400	flex	575	288
L8	146	1.49	50.5	400	flex	640	320
L9	146	1.24	57.6	0	shear	815	489
L10	146	1.49	59.3	200	shear	815	445
L11	146	1.49	43.1	350	local	615	313
L12	146	1.49	43.6	150	local	655	364
L13	146	1.49	44.1	350	punch	700	357

APPENDIX B

Detailed calculations for the strip model

Table B1 gives the detailed calculated quantities needed to develop a shear-moment capacity envelope using the strip model. Envelopes in the body of the paper are based on average quantities rather than those of any particular specimen.

Table B1: Detailed calculated quantities for strip model. Conversion: 1 kN·m = 0.74 kip·ft; 1 kN/m = 0.07 kip/ft. Std. refers to the standard reinforcement configuration, and enh. to the enhanced configuration.

		Interior Strip (top steel)		Interior Strip (bottom steel)		Spandrel Strip (top steel)		
Test	**Reinf. Config.**	M_{s2} (kN·m)	M_{ss2} (kN·m)	M_{s2} (kN·m)	M_{ss2} (kN·m)	M_{s1} (kN·m)	M_{ss1} (kN·m)	q_c (kN/m)
L1	**Std.**	27.1	54.8	44.7	85.1	44.7	69.3	142
L2	**Std.**	26.8	53.9	44.2	83.2	44.2	68.1	150
L3	**Std.**	26.8	54.0	44.2	83.4	44.2	68.2	151
L4	**Std.**	26.9	54.2	44.3	83.9	44.3	68.5	152
L5	**Std.**	27.0	55.2	44.8	86.6	44.8	69.9	161
L6	**Std.**	27.1	55.3	44.9	86.9	44.9	70.1	162
Average		26.9	54.5	44.5	84.8	44.5	69.0	155
L7	**Enh.**	27.0	55.0	57.6	108.9	44.7	69.6	169
L11	**Enh.**	26.8	54.0	56.8	104.0	44.2	68.2	160
L12	**Enh.**	26.8	53.7	56.5	102.3	44.0	67.7	158
Average		26.9	54.3	57.0	105.2	44.3	68.6	162
L9	**Std. + Studs**	27.2	56.2	45.3	89.1	45.3	71.2	170
L10	**Enh. + Studs**	27.2	56.4	58.9	116.4	45.4	71.5	184
L8	**Enh. + Hoops***	27.0	55.1	57.7	95.7	44.7	69.7	170
L13	**Enh. + Hoops***	26.8	53.8	56.6	102.9	44.1	67.9	158

For convenience, Figure B1 shows an adaptation of Fig. 4 to reflect the support conditions of the tests and the sign convention used in Albuquerque et al (2016). As the specimens are loaded symmetrically, the spandrel shears and moments on the two c_1 faces will be equal. In the absence of any special treatment to enhance capacity, the torsional moments on these faces are taken as zero.

Because the specimens are statically determinate, there can be no redistribution of moments. The eccentricity of loading at the edge column is fixed and cannot change. Equation (3) is re-written to provide an additional constraint on the forces and moments (positive sense as shown in Fig. B1) transferred between slab and column. Considering rotational equilibrium about an axis parallel to the free edge gives:

$$V_{tot} \times ecc + V_2 \times \frac{c_1}{2} = M_{face} \qquad \text{(B1)}$$

Point A:

- fully-developed interior super strip with top steel in tension
- one-way gravity shear on spandrel (c_1) faces

$$V_2 = P_{ss2} = \sqrt{\frac{2M_{ss2}q_c(1+\chi)^2}{1+\chi^2}} = \sqrt{\frac{2 \times 54.5\ kN \cdot m \times 155\frac{kN}{m} \times (1+1)^2}{(1+1^2)}} = 183.8\ kN$$

$$V_1 = 2 \times c_1 \times q_c = 2 \times 0.3\ m \times 155\ \frac{kN}{m} = 93.0\ kN$$

$V_{tot} = V_2 + V_1 = 183.8\ kN + 93.0\ kN = 276.8\ kN$

$M_{face} = -M_{ss2} = -54.5\ kN \cdot m$

From Equation (B1):

$M_{col} = V_{tot} \times ecc = M_{face} - V_2 \times \frac{c_1}{2} = -54.5\ kN \cdot m - 183.8\ kN \times \frac{0.3m}{2} = -82.1\ kN \cdot m$

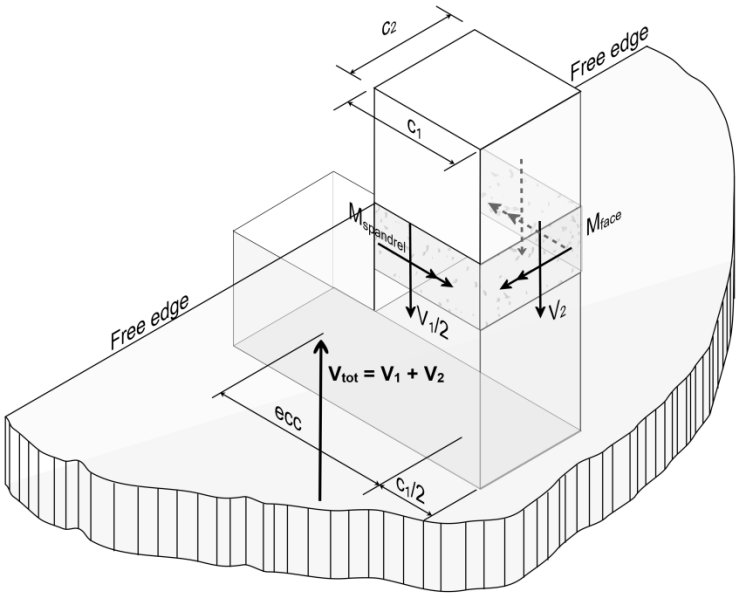

Figure B1: Forces and moments at connection

Point A':

- Common with point A: fully-developed interior super strip with top steel in tension. Hence:
  $V_2 = 183.8\ kN$; $M_{face} = -M_{ss2} = -54.5\ kN \cdot m$; and $M_{col} = -82.1\ kN \cdot m$
- Change from point A: One-way uplift shear on the spandrel (c_1) faces. Hence:
  $V_1 = -93.0\ kN$
  $V_{tot} = V_2 + V_1 = 183.8\ kN - 93.0\ kN = 90.8\ kN$

Point B:

- Fully-developed spandrel super-strips
- Maximum sagging (positive) moment from reinforcement perpendicular to the free edge.
- One-way gravity shear on the interior (c_2) face

Here we need to check whether the test specimen is wide enough to accommodate fully-developed spandrel super-strips. From Fig. 10, the maximum possible length of a spandrel super-strip is (1700 mm – 300 mm) / 2 = 700 mm. From Equation 2, the loaded length of the fully-developed super-strip is:

$$l_{ss} = \sqrt{\frac{2M_{ss1}}{q_c(1+\chi^2)}} = \sqrt{\frac{2 \times 69.0\ kN \cdot m}{155\frac{kN}{m}\ (1+0^2)}} = 0.944\ m = 944\ mm > 700\ mm$$

Since the loaded length of a fully-developed super-strip would exceeds the available length, the capacity of the spandrel arches is capped by the one-way shear strength of the slab. Hence:

$V_1 = 2 * q_c \cdot 0.7\ m = 217.0\ kN$

From Table 2, the maximum sagging moment that can be developed at the inside face of the column is 84.8 kN·m. Hence:

If: $M_{face} = 84.8 kN \cdot m$

Then: $V_2 = c_2 \times q_c = 0.3\ m \times 155 \frac{kN}{m} = 46.5\ kN$

$V_{tot} = V_1 + V_2 = 217.0\ kN + 46.5\ kN = 263.5\ kN$

$M_{col} = M_{face} - V_2 \times \frac{c_1}{2} = 84.8\ kN \cdot m - 46.5\ kN \times \frac{0.3m}{2} = 77.8\ kN \cdot m$

Point B':

- Common with point B: Fully-developed spandrel super-strips and maximum sagging (positive) moment from reinforcement perpendicular to the free edge. Hence:
  $V_1 = 217.0\ kN$ and $M_{face} = 84.8 kN \cdot m$
- Change from Point B: One-way uplift shear on the interior (c_2) face. Hence:
  $V_2 = -46.5\ kN$;

$V_{tot} = V_1 + V_2 = 217.0\ kN - 46.5\ kN = 170.5\ kN$

$M_{col} = M_{face} - V_2 \times \frac{c_1}{2} = 84.8\ kN \cdot m + 46.5\ kN \times \frac{0.3m}{2} = 91.8\ kN \cdot m$

Point C:

- Proportional loading: Spandrel and interior arch strips with restricted values of $M_{s,col}$ for all.

As was case for point B, need to check if specimen is wide enough to allow spandrel arch strip.

$l_s = \sqrt{\frac{2M_{s1}}{q_c(1+\chi^2)}} = \sqrt{\frac{2 \times 44.5\ kN \cdot m}{155 \frac{kN}{m}\ (1+0^2)}} = 0.758\ m = 758\ mm > 700\ mm$

The loaded length of a conventional arch strip exceeds the available length. Hence:

$V_1 = 2 * q_c \cdot 0.7\ m = 217.0\ kN$

$V_2 = P_{s2} = \sqrt{\frac{2M_{s2}q_c(1+\chi)^2}{1+\chi^2}} = \sqrt{\frac{2 \times 26.9\ kN \cdot m \times 155 \frac{kN}{m} \times (1+1)^2}{(1+1^2)}} = 129.1\ kN$

$V_{tot} = V_1 + V_2 = 217.0\ kN + 129.1\ kN = 346.1\ kN$

$M_{face} = -M_{s2} = -26.9\ kN \cdot m$

$M_{col} = M_{face} - V_2 \times \frac{c_1}{2} = -26.9\ kN \cdot m - 129.1\ kN \times \frac{0.3m}{2} = -46.2\ kN \cdot m$

Point D:

- Similar to point B except moment on inside face is hogging (negative) rather than sagging
- Fully-developed spandrel super-strips

- One-way gravity shear on the interior (c_2) face
- Find value of hogging moment at interior face for which the load carried by an arch strip matches the load carried by one-way shear. an arch strip one-way shear and that would Maximum hogging moment from reinforcement perpendicular to the free edge.

  As before:

  $V_1 = 2 * q_c \cdot 0.7\ m = 217.0\ kN$

  $V_2 = \ c_2 \times q_c = 0.3\ m \times 155 \frac{kN}{m} = 46.5\ kN.$

  $V_{tot} = V_1 + V_2 = 217.0\ kN + 46.5\ kN = 263.5\ kN$

  Find transition moment, determined by value of hogging moment at interior face for which the load carried by an arch strip matches the load carried by one-way shear. From rearranged equation 2:

$$M_{s2,tran} = \frac{P_{s2,tran}^2 \times (1+\chi^2)}{2 \times q_c \times (1+\chi)^2} = \frac{(46.5kN)^2 \times (1+1^2)}{2 \times 155 \frac{kN}{m} \times (1+1)^2} = 3.49\ kN \cdot m$$

  Hence:

  $M_{face} = -3.49\ kN \cdot m$

$$M_{col} = M_{face} - V_2 \times \frac{c_1}{2} = -3.49\ kN \cdot m - 46.5\ kN \times \frac{0.3m}{2} = -10.46\ kN \cdot m$$